JOURNAL OF VIROLOGY, May 2002, p. 4591–4602 Vol. 76, No. 9
0022-538X/02/$04.00+0 DOI: 10.1128/JVI.76.9.4591–4602.2002

Rafts Promote Assembly and Atypical Targeting of a Nonenveloped Virus, Rotavirus, in Caco-2 Cells

Catherine Sapin,[1] Odile Colard,[1] Olivier Delmas,[1] Cedric Tessier,[1] Michelyne Breton,[1] Vincent Enouf,[2] Serge Chwetzoff,[1] Jocelyne Ouanich,[1] Jean Cohen,[2] Claude Wolf,[1] and Germain Trugnan[1]*

INSERM U 538, CHU Saint Antoine, Université Pierre et Marie Curie, 75012 Paris,[1] and Virologie Moléculaire et Cellulaire, INRA, 78352 Jouy en Josas,[2] France

Received 1 October 2001/Accepted 22 January 2002

Rotavirus follows an atypical pathway to the apical membrane of intestinal cells that bypasses the Golgi. The involvement of rafts in this process was explored here. VP4 is the most peripheral protein of the triple-layered structure of this nonenveloped virus. High proportions of VP4 associated with rafts within the cell as early as 3 h postinfection. In the meantime a significant part of VP4 was targeted to the Triton X-100-resistant microdomains of the apical membrane, suggesting that this protein possesses an autonomous signal for its targeting. At a later stage the other structural rotavirus proteins were also found in rafts within the cells together with NSP4, a nonstructural protein required for the final stage of virus assembly. Rafts purified from infected cells were shown to contain infectious particles. Finally purified VP4 and mature virus were shown to interact with cholesterol- and sphingolipid-enriched model lipid membranes that changed their phase preference from inverted hexagonal to lamellar structures. Together these results indicate that a direct interaction of VP4 with rafts promotes assembly and atypical targeting of rotavirus in intestinal cells.

Lipids membrane microdomains are dynamic entities involved in the control of the lipid-lipid and lipid-protein interactions that play a key role in numerous cellular functions such as signal transduction and membrane transport and trafficking (27). Membrane microdomains enriched in cholesterol and sphingolipids, also termed rafts, are thought to act as transitory platforms on which lipids and proteins may interact dynamically to exert a function that may be interrupted as the microdomain dissociates. It is thought that rafts emerge from the Golgi apparatus and reach the plasma membrane through a still-discussed intracellular pathway. Among the numerous functions of microdomains so far explored, various steps of virus interactions with their host cells have been proposed (8, 32, 44, 47, 53, 66, 71). These findings mainly concerned enveloped viruses, whose lipid membranes are expected to interact with the host cell membranes. By contrast, nonenveloped viruses that replicate and assemble in the cytoplasm of host cells have been scarcely explored for their putative interactions with membrane microdomains (37, 48).

Rotavirus, a triple-layered nonenveloped virus (70), is a worldwide cause of infantile gastroenteritis, accounting for an estimated 600,000 deaths annually (2). Knowledge of the detailed process of virus assembly is required to provide a molecular basis for the design of drugs or strategies able to interfere with virus entry, assembly, and/or replication. The interest in this approach has been enhanced since the withdrawal of the tetravalent vaccine because of side effects (7). In vivo rotavirus specifically targets highly polarized intestinal cells (59). This prompted us to develop studies on rotavirus infection of Caco-2 cells (17), which originate from human colon and which display a well-polarized and differentiated enterocytic phenotype when grown in culture (11). We demonstrated earlier that rotavirus was secreted before any significant cell lysis in a highly polarized way to the apical sides of Caco-2 cells. We also observed that virus apical secretion followed an atypical route through vesicular traffic bypassing the Golgi apparatus (30). Together, these results address the question of the precise mechanisms and localization of rotavirus assembly in these cells.

The widely accepted model for rotavirus assembly (14) was deduced from studies performed essentially with MA 104 cells, a poorly differentiated cell line originating from monkey kidney epithelium (67). The model may be summarized as follow. After solubilization of the outer capsid layer, the translation of structural and nonstructural proteins takes place in the host cell cytoplasm. A subset of structural proteins, namely, VP1, VP2, VP3, and VP6, assemble in the viroplasm, an ill-defined structure from which double-layered particles (DLP) that contain the double-stranded RNA emerge. The next step includes the translocation of DLP across the endoplasmic reticulum (ER) membrane and the formation of a transient envelope around the viral particles inside the ER lumen (49). Entry of DLP into the ER lumen is likely to be driven by specific interactions between VP6 on the DLP and the cytoplasmic domain of NSP4 (63). Exit of virus from the ER and assembly with VP7 and VP4 are less documented and involve a ternary complex containing NSP4, VP7, and VP4 (36, 60). NSP4 and VP7 are two integral transmembrane proteins tightly associated with the ER membrane (9, 50). VP7 has also been shown outside the ER in punctate structures that likely correspond to accumulated virus particles and in regions of the ER surrounding the viroplasm (31). NSP4 has also been recently identified along microtubule-like structures (69).

The present knowledge of VP4 localization is much less clear. Based on conventional electron-microscopic studies it has been assumed that VP4 may be present as a fine reticular

* Corresponding author. Mailing address: INSERM U 538, CHU Saint Antoine, 27, rue de Chaligny, 75012 Paris, France. Phone: 33 1 40011323. Fax: 33 1 40011390. E-mail: trugnan@st-antoine.inserm.fr.

material associated with VP7 and NSP4 at the junction area of the ER membrane and virus particles (60). However no obvious evidence that VP4 is in the transiently enveloped immature virus that has been observed in the ER or in any other location within the ER has been provided so far (22). Therefore it is difficult to reconcile the hypothesis of a complete intrareticular assembly of rotavirus with an exclusive extrareticular localization for VP4. Indeed, we recently showed that, early after MA 104 cell infection, VP4 was not localized within the ER but was associated with the plasma membrane, intracellular vesicles, and microtubules. Interestingly, this localization was also observed in MA 104 cells transfected with a VP4 plasmid, suggesting that VP4 targeting depends on signals present on the protein rather than on virus particles (46).

From the above data, it appears that a better knowledge of VP4 localization and targeting in polarized Caco-2 cells should provide key information on rotavirus assembly and polarized secretion. Since a previous study of ours indicates that virus particles are targeted to the apical side of the cells (30), we hypothesized that virus interacts, at least to some extent, with the apical targeting machinery of Caco-2 cells. It has been recently proposed that rafts play a pivotal role in apical sorting and targeting in polarized cells (58). Rafts have been defined by their insolubility in Triton X-100 detergent (6, 35) due to their high proportion of cholesterol, sphingolipids, and/or glycosphingolipids. It has been shown that, in Caco-2 cells, rafts are involved in the apical targeting of glycosylphosphatidylinositol (GPI)-anchored glycoproteins such as alkaline phosphatase (AP) and of some transmembrane glycoproteins such as sucrase-isomaltase (SI) but not of dipeptidyl peptidase IV (DPP IV), another apically targeted hydrolase (1, 20).

In the present study we have undertaken an extensive analysis of VP4 localization and targeting in Caco-2 cells following rotavirus infection. We searched for a putative association of VP4 with rafts. Our rationale for such an approach was based (i) on the apical targeting of viral particles in Caco-2 cells; (ii) on the observation that, in rotavirus-infected Caco-2 cells, SI targeting is impaired whereas DPP IV targeting is mostly unaffected (29); and (iii) on data indicating that rotavirus may interact with glycosphingolipids (12) highly enriched in rafts, as well as with some raft proteins (23). We found that VP4 associates with rafts within the cells as early as 3 h postinfection (p.i.), a phenomenon concomitant with an early apical targeting of VP4 to rafts located at the apical membrane of Caco-2 cells. Later on, other structural proteins also became associated with rafts, a process that leads to the assembly of mature rotavirus. These results indicate that VP4 drives the assembly of rotavirus particles by using rafts as a platform. Such a proposal implies that the final step of rotavirus assembly should take place in an extrareticular compartment, thus leading to a new model for rotavirus assembly that is the first example of the implication of rafts in the intracellular handling of a nonenveloped virus.

MATERIALS AND METHODS

Cells and infection. Caco-2 cells (passages 50 to 70) were cultured as previously described (11) in Dulbecco's modified Eagle medium (DMEM) supplemented with 20% heat-inactivated (56°C, 30 min) fetal calf serum (FCS), 1% nonessential amino acids, and 100 U of penicillin and 100 μg of streptomycin/ml (all reagents were from Life Technologies, Cergy Pontoise, France). Cells were grown at 37°C in a 10% CO–90% air atmosphere. For cell maintenance, cells were seeded at 6×10^3 cells per cm^2 in 25-cm^2 plastic flasks (Corning Costar France, Brumath, France). Cells were changed daily and were passaged each week. To allow separate access to the apical and basolateral sides of cell monolayers, cells were grown on tissue culture-treated polycarbonate Transwell filters (Corning Costar France) with a 12-mm diameter and 0.4-μm pore size at a density of 10^4 cells per filter. MA 104 cells were cultured in DMEM supplemented with 10% FCS and penicillin and streptomycin (100 U/ml and 100 μg/ml, respectively), as previously described (46). Caco-2 cells were infected with rotavirus RF strain (34) at day 21 after seeding, as previously described (30). Briefly, cells were cultured at least for 6 h without FCS in modified Eagle medium buffered with 20 mM HEPES, pH 7.6. Cells were then incubated in the presence of a trypsin-preactivated rotavirus suspension adjusted to 10 PFU/cell at 4°C for 1 h. After three washes in a medium containing 0.5 μg of trypsin/ml without FCS, cells were maintained at 37°C for various p.i. periods. Infectious titers of the RF strain on MA 104 cells were determined as previously described (46).

Transfection. Caco-2 cells were transfected with a supercoiled DNA plasmid encoding VP4-green fluorescent protein (GFP) (46). Transfections were performed using FuGENE 6 (Roche Diagnostics, Meylan, France) according to the manufacturer's instructions. Briefly, Caco-2 cells were seeded in six-well plates (10^5 per well). Two days later, transfection was performed at around 60% confluence. Cells were washed twice with OptiMEM. Five micrograms of supercoiled DNA was gently mixed with 12.5 μl of transfection reagent in 1 ml of OptiMEM (Life Technologies). Cells were transfected for 6 h, washed three times, and observed within 48 h posttransfection.

DRM preparation. Detergent-resistant membranes (DRM) were prepared on ice as follows. Cells were washed twice with phosphate-buffered saline (PBS), scraped in TNE buffer (20 mM Tris-HCl [pH 7.4], 150 mM NaCl, 1 mM EDTA, and a mixture of antiproteases: 4 mM 4-[2-aminoethyl]-benzenesulfonyl fluoride [AEBSF] and 25 μg of benzamidine, 10 mg of aprotinin, 10 μg of antipain, 10 μg of leupeptin, and 10 μg of pepstatin/ml) containing 1% Triton X-100, passed 10 times through a 22-gauge needle, and kept at 4°C for 30 min. Triton X-100-treated homogenates were then mixed with sucrose or OptiPrep (Sigma-Aldrich, St. Quentin Fallavier, France) such that density reached 40%. DRM were separated from detergent-solubilized membranes and from soluble proteins by ultracentrifugation either on a discontinuous (40, 35, and 5%) sucrose gradient (180,000 × *g* for 18 h at 4°C in a Beckman SW 41 rotor) or on a discontinuous (40, 30, and 5%) OptiPrep gradient (100,000 × *g* for 4 h at 4°C in the same rotor). In both protocols, DRM were recovered in fractions 4 and 5 at the interface of the 5% layer with the 30 or 35% layer. After vigorous mixing, the 40% layer was considered the soluble fraction. Triton X-100 homogenates were sonicated before being analyzed.

Lipid analysis. Lipids from DRM and whole-cell homogenates were extracted in chloroform-methanol following phase separation as described by Bligh and Dyer (4). Solvents were removed under a stream of nitrogen, and the lipids were resuspended in chloroform-methanol (1:1 [vol/vol]). Total phospholipids were determined on crude lipid extract by measurement of phosphorus content. Separation of the main classes of phospholipids was achieved by thin-layer chromatography (TLC) in chloroform-methanol-water (65:25:4 [vol/vol]). Sphingomyelin was scraped from the plate and assayed for phosphorus content. For cholesterol determination, an aliquot of lipid extract was evaporated and redissolved in ethanol. Cholesterol content was determined by a colorimetric assay (19).

HPLC analysis of phospholipid molecular species. Total phospholipids were separated from neutral lipids by loading lipid extracts on TLC plates and developing them in petroleum ether-ethyl ether-acetic acid (70:30:1 [vol/vol/vol]). Phospholipids were scraped from the plate, extracted from silica gel, and hydrolyzed by phospholipase C from *Bacillus cereus* (Sigma-Aldrich), and the diglycerides obtained were converted to benzoylated derivatives (3). These derivatives absorb at 230 nm, and the absorption is proportional to their amounts. After purification by TLC, the molecular species were analyzed by reverse-phase high-pressure liquid chromatography (HPLC; acetonitrile–propanol-2 [75/25 {vol/vol}]), and peaks were visualized by absorption at 230 nm as already described (38).

Antibodies. A rabbit polyclonal anti-RF antiserum (8148) that recognized VP2, VP4, VP6, and VP7 was diluted 1:400 for immunofluorescence (IF) and 1:3,000 for Western blot (WB) analysis. A mouse monoclonal anti-VP4 antibody (7.7) that is directed against VP8* and that also recognizes VP4 in mature virus was used at 1:200 (IF) or 1:1,000 (WB) (46). A mouse monoclonal anti-VP2 antibody (164E22) was used at 1:1,000 (52). A rabbit polyclonal antibody raised against NSP4 (1:1,000) was a gift from J. Taylor (Auckland, New Zealand). A rat monoclonal anti-human DPP IV (1:200) was a gift from S. Maroux (Marseille, France). A mouse monoclonal anti-human SI (1:200) was a gift from H.-P. Hauri

(Basel, Switzerland). A mouse monoclonal anti-human AP (clone 8B6; 1:300 for IF and 1:1,000 for WB) was purchased from Sigma-Aldrich. Fluorescein-conjugated donkey anti-rabbit immunoglobulin G (IgG), donkey anti-mouse IgG, and donkey anti-rat IgG (Jackson Laboratories, Interchim, Montluçon, France) were used at 1:200. Peroxidase-conjugated donkey anti-rabbit IgG and anti-mouse IgG (Pierce, Interchim) were used at 1:15,000.

IF and confocal microscopy. Caco-2 cells, grown either on glass coverslips or on filters, were washed three times with cold PBS and then fixed with 2% paraformaldehyde (PFA) for 20 min at room temperature. All the subsequent steps were carried out in the presence of 50 mM NH_4Cl to quench free aldehyde groups. When indicated, cells were permeabilized with saponin (0.075%). Saponin was added in all the subsequent solutions. Permeabilized and nonpermeabilized cells were incubated with the primary antibody for 45 min at room temperature. After three washes with PBS, the second fluorescence-labeled antibody was incubated for 30 min at room temperature. Cells were washed five times with PBS and, in some experiments, incubated with 1 mg of RNase A/ml for 10 min and with propidium iodide (1 μg/ml) for 3 min to visualize nuclei. Samples were treated with 100 mg of diazabicyclo[2.2.2.]octane (DABCO; Sigma-Aldrich)/ml and mounted with Glycergel (Dako SA, Trappes, France). Fluorescence was observed with a Leica TCS Spectral (SP1) equipped with a DMR inverted microscope and 63× and 40× objectives, both with a numerical aperture of 1.4. A krypton-argon mixed-gas laser was used to generate two bands: 488 nm for fluorescein isothiocyanate (FITC) and 568 nm for propidium iodide. Image processing was performed using the on-line Scan Ware software. Numeric images, stored on compact disk, were treated and mounted on an image analysis station (Scion Image and Photoshop, version 5.1).

WB analysis. After trichloroacetic acid (TCA) precipitation, proteins recovered from gradients were separated by sodium dodecyl sulfate–7.5 or 10% polyacrylamide gel electrophoresis together with molecular weight standards (Amersham Pharmacia Biotech, Saclay, France) and transferred onto nitrocellulose (Hybond-C; Amersham). Nonspecific staining was prevented by 2 h of incubation in a polyvinylpyrrolidone (PVP) solution (1% PVP, 0.05% Tween 20 in PBS). Nitrocellulose sheets were incubated with a primary antibody for 1 h at room temperature. After five washes with PBS-Tween 20, the second antibody was added for 1 h at room temperature. After five washes, the ECL reagent (Amersham) and Biomax-Light 1 films (Kodak, Sigma-Aldrich) were used to reveal proteins. Films were scanned with a densitometric scanner (Agfa), and bands were quantified with Scion Image software.

X-ray diffraction analysis. The small-angle scattering data were recorded at station 8.2 of SRS Daresbury Laboratory (Warrington, United Kingdom; beam time EC allocation 36039). Twenty milligrams of lipids, obtained from Sigma-Aldrich, was fully hydrated (>1/1 [wt/wt]) with an aqueous buffer (10 mM Tris-HCl, pH 8.0) containing calcium in a 1/1,000 to 1/100 molar ratio with lipid. The virus particles (20 mg of purified trypsinized virus particles/ml) (18) or the viral protein (1 mg of purified VP4/ml recovered after expression in *Escherichia coli* as a fusion protein with a His tag using plasmid vector pET-28b(+) from Novagen [Tebu, Le Perray en Yvelines, France] and purified with chelating Sepharose-nickel from Amersham) was mixed with lipids during the hydration step. To insure a homogeneous hydration, the sample was sealed under argon for at least a week before X-ray examination. The camera length was set to 2.5 m. The response of the quadrant detector was recorded with radioactive source ^{59}Fe, allowing the normalization of scattering records for the channel response (1,024 channels/frame). The temperature was varied linearly with a programmable stage (Linkham) during the measurement. The data were processed with Otoko software kindly provided by M. Koch (5).

RESULTS

Early after rotavirus infection, VP4 is specifically expressed at the apical membrane of Caco-2 cells. As a starting point to study VP4 localization in infected Caco-2 cells, indirect IF and confocal microscopy were used. Confluent, differentiated Caco-2 cells, grown on filters, were infected with the RF rotavirus strain at 10 PFU/cell and were analyzed 3, 6, 12, and 18 h p.i. To visualize VP4, monoclonal antibody 7.7 was applied on both sides of the filter. This antibody recognizes VP4 in rotavirus particles as well as native VP4 (46). VP4 was detectable in infected cells as soon as 3 h p.i. (not shown). In nonpermeabilized cells, VP4 staining was restricted to the apical membrane. As shown in Fig. 1A, all infected cells displayed a strong apical staining that became obvious at 6 h p.i. To further analyze this localization, higher magnification was used (Fig. 1B) and *xz* sections (Fig. 1C) were examined; this confirmed the lack of basolateral staining. The apical staining was present at all the times studied. When cells were permeabilized, intracellular structures were also stained, either as intracellular vesicles of heterogeneous size or as microtubular structures (Fig. 1D and E), reminiscent of our recently published results on MA 104 cells (46). Since these structures were stained early

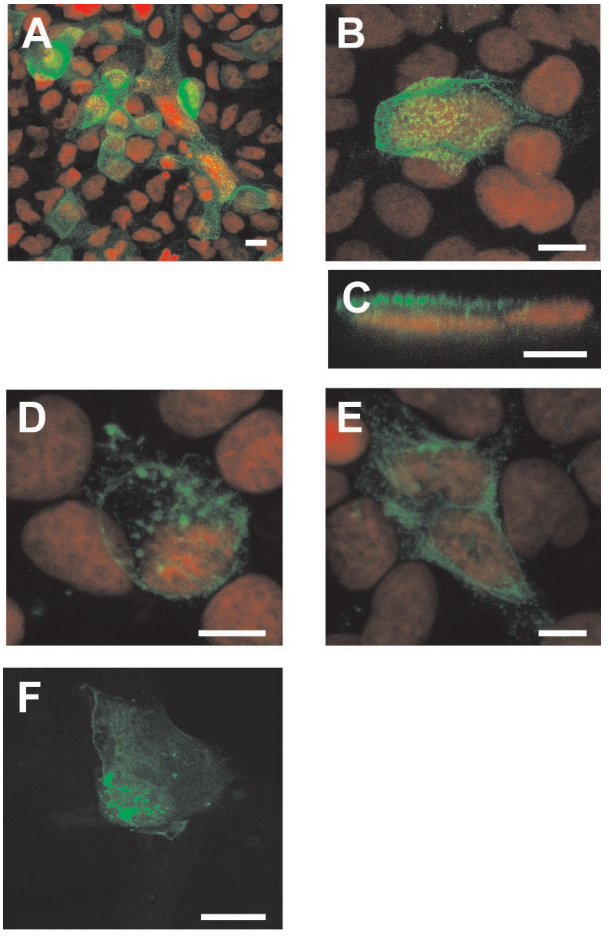

FIG. 1. Early after rotavirus infection, VP4 is expressed at the apical membrane of Caco-2 cells and in discrete intracellular locations. Caco-2 cells (21 days old), grown on Transwell filters, were infected with the RF rotavirus strain at 10 PFU/cell (A to E). Six hours p.i., cells were fixed with 2% PFA and not permeabilized (A to C) or permeabilized (D and E). VP4 was detected using monoclonal antibody 7.7 and a FITC-labeled secondary anti-mouse IgG antibody. Nuclei were labeled with propidium iodide (red channel). (A) General representative view of the sum of the five most apical sections (1 μm deep each). (B) *xy* projection on a zoomed view. Ten 0.5-μm-thick sections were recorded from the top to the bottom and were projected on one plane to recover all the data available in the sample. (C) *xz* section obtained through an *xz* direct scanning procedure. (D and E) In permeabilized cells, it was possible to show that VP4 localized to discrete locations that evoked vesicular and tubular structures, which are illustrated as 1-μm-thick sections through the middle of the cells. (F) Cells were transiently transfected with VP4-GFP, as described in Materials and Methods, and directly observed with the confocal microscope within 48 h posttransfection. A sum of 15 sections, each 0.5 μm thick, is displayed. Bars = 10 μm.

after infection, this suggested that the VP4 protein possesses autonomous signals that drive it to its different locations independently of the expression of other rotavirus structural proteins. To confirm this point, Caco-2 cells were transiently transfected with a VP4-GFP construct (46). As shown in Fig. 1F, this chimeric protein was found to be expressed at the plasma membrane, as well as in intracellular vesicles and along microtubular structures. As mentioned above for infected cells, the localization of VP4 in transfected cells may vary from one cell to another, a phenomenon that may due to the fact that VP4 by itself may perturb cell organization in a time-dependent manner and have a "toxic" effect (S. Chwetzoff et al., unpublished data). This phenomenon is associated with a quite low transfection efficiency and with the fact that only transient expression may be analyzed. In any case, the three main localizations found in infected cells were also observed in transfected cells. The plasma membrane localization especially was clearly visible on individual optical sections (not shown). It is interesting that VP4, which is synthesized as a cytosolic protein lacking an obvious transmembrane domain, was never present in the cytosol but rather displayed a strict compartmentalized subcellular distribution. These observations suggested that VP4 should interact with host cellular membranes and/or proteins to achieve this specific distribution.

Apically expressed VP4 is mainly in Triton X-100-resistant microdomains. VP4 is strongly expressed at the apical membrane, and we hypothesized that this may be due to an interaction with rafts that have been involved in the apical targeting of membrane proteins in Caco-2 cells (20). Therefore, to demonstrate a putative association of VP4 with rafts, we performed experiments in which infected Caco-2 cells were extracted with Triton X-100 and analyzed by indirect IF and confocal microscopy for the presence of proteins that resist this extraction. SI and AP were selected as positive controls, and DPP IV was used as negative control. As expected, both SI (Fig. 2A to D) and AP (Fig. 2E and F) were present at the apical membrane both before (Fig. 2A, B, and E) and after (Fig. 2C, D, and F) exposure to Triton X-100, whereas DPP IV was present before (Fig. 2G and H) but not after (Fig. 2 I and J) Triton X-100 extraction. As shown in Fig. 2K to N VP4 displayed a pattern similar to those of SI and AP, i.e., present both before (Fig. 2K and L) and after (Fig. 2M and N) Triton X-100 extraction, thus indicating that this protein was associated with rafts at the apical membrane of Caco-2 cells.

VP4 is present in Triton X-100-resistant membranes purified from infected Caco-2 cells. As VP4 is observed in Triton X-100-resistant patches in the apical membrane, we wondered whether this association occurs in the plasma membrane or, more likely, within the cell, where lipid microdomains and proteins associated. To investigate this point, the presence of VP4 in Triton X-100-resistant microdomains prepared 18 h p.i. was tested by a biochemical approach. Infected Caco-2 cells were treated with 1% Triton X-100 at 4°C for 30 min, and the DRM were isolated after flotation on a sucrose gradient. Each fraction was analyzed by sodium dodecyl sulfate-polyacrylamide gel electrophoresis and Western blotting using monoclonal antibody 7.7 against VP4. As shown in Fig. 3, a significant proportion of VP4, corresponding to the density of DRM, was associated with fractions 4 and 5, which correspond to the density of DRM containing AP (Fig. 3). It should be men-

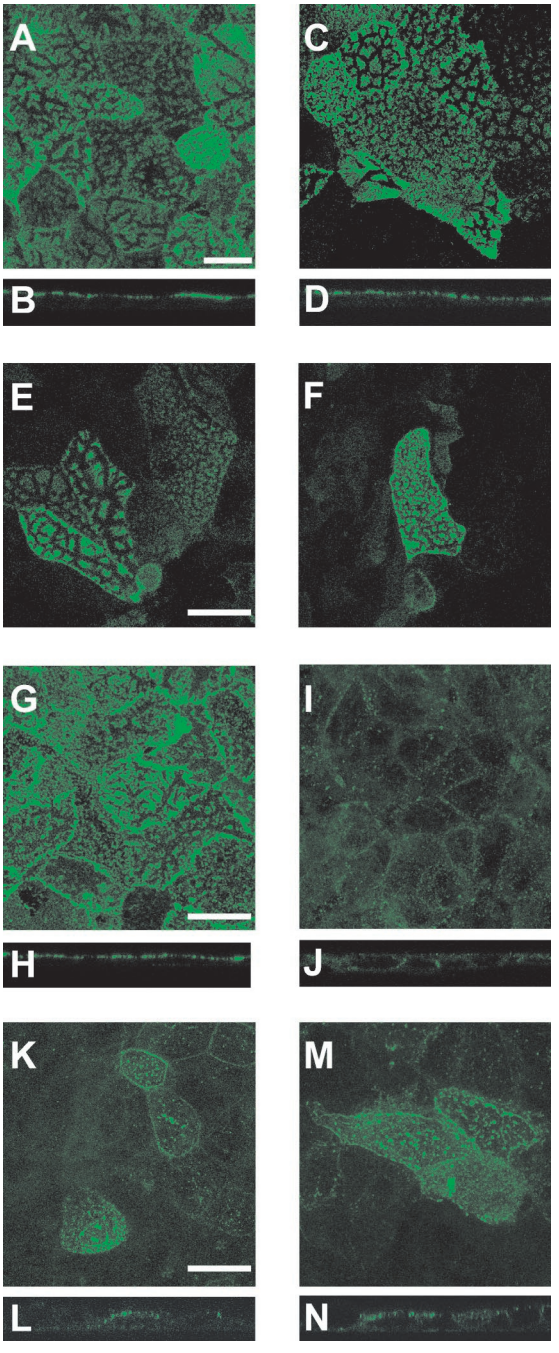

FIG. 2. Apically expressed VP4 resists Triton X-100 extraction. Caco-2 cells (21 days old), grown on glass coverslips, were infected with the RF rotavirus strain at 10 PFU/cell. Six hours p.i., cells were extracted with Triton X-100 on ice for 1 to 2 min, fixed with 2% PFA, and analyzed by indirect IF and confocal microscopy for the presence of proteins that do or do not resist detergent extraction. SI (A to D) and AP (E and F) were selected as positive controls, and DPP IV (G to J) was used as a negative control. VP4 (K to N) was revealed using monoclonal antibody 7.7. Twenty-five 0.5-μm-thick sections were recorded and combined (projection) to obtain an *xy* representation of SI (A and C), AP (E and F), DPP IV (G and I), and VP4 (K and M). *xz* sections were obtained through an *xz* direct-scanning procedure for SI (B and D), DPP IV (H and J), and VP4 (L and N). Panels A, B, E, G, H, K, and L were obtained in the absence of Triton X-100, whereas panels C, D, F, I, J, M, and N were recorded after Triton X-100 extraction. Bars, 10 μm.

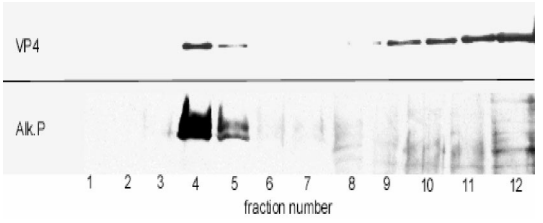

FIG. 3. VP4, the spike protein of rotavirus, is present in the DRM fraction. Caco-2 cells infected with rotavirus (10 PFU/cell) were treated with 1% Triton X-100 on ice 18 h p.i., and DRM were floated on a sucrose gradient as described in Materials and Methods. Twelve fractions were collected, fraction 1 representing the top of the gradient. Aliquots of each fraction were precipitated with TCA, and the distribution of rotavirus VP4 and AP along the gradient was assayed by immunoblotting.

tioned that caveolin, the archetypal marker of rafts, was not used here because both caveolin 1 and 2 are not expressed in Caco-2 cells (40).

Rotavirus infection does not modify the lipid composition of rafts in Caco-2 cells. It has been assumed that assembly of lipid molecules into rafts is dynamic and depends on associated proteins (27). It was therefore relevant to determine whether or not rotavirus infection modified the raft lipid composition. A detailed analysis of the lipid compositions of whole-cell membranes and isolated DRM in both control and infected cells was performed. Table 1 shows that the recovery of cholesterol and sphingomyelin in the DRM fraction of control and infected cells was about three times higher than the recovery of the glycerophospholipids. This enrichment in cholesterol and sphingomyelin is comparable to what has been previously observed in several other cell systems (28, 41). DRM prepared from rotavirus-infected Caco-2 cells were not significantly different (Table 1).

The glycerophospholipids present in DRM are enriched in saturated and monounsaturated fatty acids (51, 55). Analysis of the phospholipid molecular species composition of infected and noninfected DRM performed by HPLC has confirmed this particularity. As shown in Fig. 4 and Table 2, the levels of diunsaturated species such as the dioleoyl in DRM were decreased relative to the levels in total membranes. In contrast,

TABLE 1. Cholesterol and sphingomyelin content of DRM from Caco-2 cells is not modified by rotavirus infection[a]

Lipid	Content[b] (nmol/mg of protein in homogenate [%]) in:	
	Infected cells	Mock-infected cells
Cholesterol	13.7 ± 1.4 [32]	14.2 ± 1.6 [32]
Sphingomyelin	6.1 ± 1.5 [29]	6.7 ± 1.1 [33]
GPL	20.4 ± 2.2 [10]	21.5 ± 1.9 [11]

[a] Flasks of Caco-2 cells (75 cm^2) were infected with rotavirus or mock infected. At 18 h p.i. DRM were prepared on a sucrose gradient as for Fig. 3. Lipids from whole-cell homogenates and DRM fractions were extracted with chloroform-methanol as described in Materials and Methods.

[b] Results are means ± standard deviations from three independent experiments. Percentages (in brackets) were derived by dividing the amount of a given lipid in the DRM fraction by the amount of the same lipid in the whole-cell homogenate. Cholesterol was assayed from the lipid extract by a colorimetric assay. Glycerophospholipids (GPL) and sphingomyelin were quantified by phosphorus assay, sphingomyelin being assayed after TLC separation.

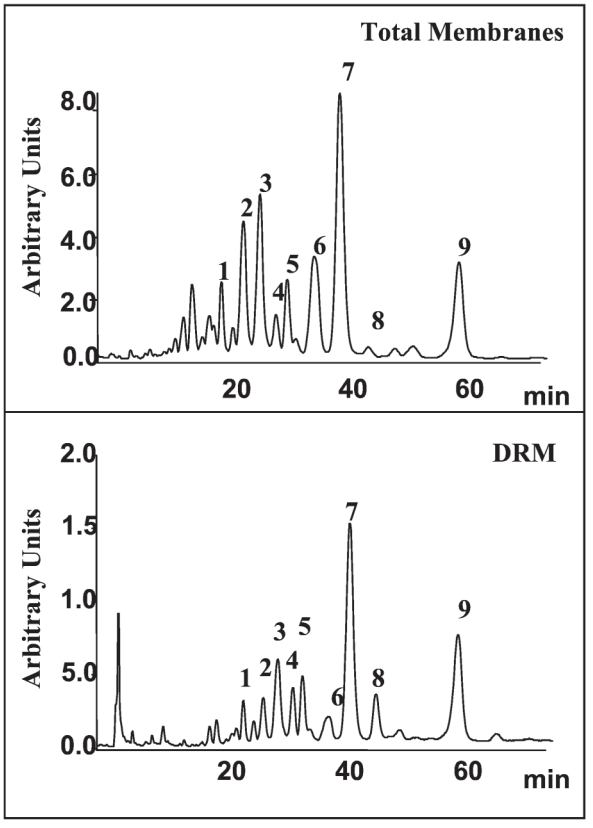

FIG. 4. HPLC profile of glycerophospholipid molecular species in the total membrane and DRM from Caco-2 cells. The glycerophospholipids isolated from total membranes or DRM of Caco-2 cells were treated with phospholipase C, and the diglycerides obtained were benzoylated as described in Materials and Methods. These derivatives were analyzed by HPLC using an RP-C18 column and a mixture of acetonitrile–isopropan-2-ol (75/25 [vol/vol]) and quantified through their absorption at 230 nm. Peak identification has been already described (38) and is reported on Table 2.

levels of disaturated species such as dipalmitoyl and monounsaturated species such as the palmitoyl-oleoyl and stearoyl-oleoyl species of phosphatidylcholine were increased more than threefold. As shown in Table 2, rotavirus infection did not modify this composition.

The glycosphingolipids present in DRM were also analyzed. No significant differences between DRM prepared from infected and noninfected cells were observed (data not shown).

VP4 is enriched in Triton X-100-resistant membranes purified from infected Caco-2 cells. A significant part of VP4 was recovered in the pellet from the sucrose gradient together with AP. This pellet also contained large amounts of cholesterol and sphingomyelin. To improve the recovery of VP4 present in DRM, OptiPrep gradients were performed; this allowed flotation of most of the DRM fraction. VP4 contents in total-DRM and soluble fractions at different times p.i. were then compared. As shown in Fig. 5A, VP4 was present in DRM and soluble fractions from 6 h p.i. and its amount increased until 18 h p.i (Fig. 5B). Quantification of blots showed that the amount of VP4 associated with DRM was rather constant with time (40.5% ± 5.9%, $n = 8$). Since the DRM fraction con-

TABLE 2. Glycerophospholipid molecular species composition of rafts from Caco-2 cells is not modified by rotavirus infection[a]

Peak[b]	Molecular species[c]	% of total species[d] in:			
		Mock-infected-cell:		Infected-cell:	
		Ho	DRM	Ho	DRM
1	16:0/20:4	5.3	1.4	4.6	1.4
2	16:1/18:1, 18:1/18:2	8.0	4.3	8.9	4.3
3	16:0/16:1, 16:0/18:2	10.9	9.6	11.3	9.0
4	nd[e]	2.3	4.5	2.0	4.4
5	18:0/20:4	5.0	4.9	4.7	4.6
6	18:1/18:1	10.6	4.6	11.9	4.5
7	16:0/18:1, 18:0/18:2	26.0	32.4	24.2	31.8
8	16:0/16:0	1.3	4.0	0.9	3.2
9	18:0/18:1	10.9	23.0	11.7	24.7

[a] The glycerophospholipids isolated from total membranes (Ho) and DRM of infected and mock-infected Caco-2 cells were treated as for Fig. 4.
[b] Peak numbers refer to Fig. 4.
[c] Molecular species are identified as follows: the first figure corresponds to the number of carbons in the fatty acid, and the second figure indicates the number of double bonds. 16:0, palmitic acid; 16:1, palmitoic acid; 18:0, stearic acid; 18:1, oleic acid; 18:2, linoleic acid; 20:4, arachidonic acid.
[d] Data are representative of two independent experiments.
[e] nd, not determined.

tained about eightfold less protein than the soluble fraction, this corresponded to a fourfold VP4 enrichment in the DRM relative to the soluble fraction (Fig. 5C).

VP4 interacts with model membranes containing cholesterol and sphingolipids and alters the physical arrangement of lipids in quaternary mixtures. Since a significant proportion of VP4 was associated with membrane microdomains enriched in cholesterol and sphingolipids upon viral infection and since VP4 does not present any known signature for membrane association, the question of whether this interaction was direct or indirect was raised. To address this question, in vitro experiments using X-ray diffraction were carried out to challenge the putative interactions of recombinant purified VP4 with a model lipid membrane resembling rafts by its abundance in sphingomyelin and cholesterol. It is a phase-sensitive model designed for X-ray diffraction examination consisting of a lipid mixture which contains aminoglycerophospholipids phosphatidylethanolamine and phosphatidylserine, sphingomyelin, and cholesterol in the ratio 4/1/2/2. This critical proportion insures an inverted-hexagon arrangement (HII) over the whole range of temperatures investigated (14 to 45°C) (Fig. 6A). The phase behavior of such a quaternary mixture as a function of temperature was previously characterized (68). The physical arrangement of this quaternary mixture is known to be sensitively influenced by the opposite phase preference of the aminoglycerophospholipids for HII and of sphingomyelin for a lamellar arrangement. As seen in Fig. 6A the interaction of cholesterol with sphingomyelin favors the hexagonal arrangement with a repeat distance of 6.40 nm in the absence of VP4. When the purified VP4 protein was added to the quaternary mixture phosphatidylethanolamine-phosphatidylserine-sphingomyelin-cholesterol, the phase preference of the lipid mixture was shifted to a single lamellar arrangement. The lamellar arrangement was maintained up to 37°C and coexisted up to the highest temperature of the range investigated (45°C) with the hexagonal arrangement (Fig. 6B). These data favored the idea

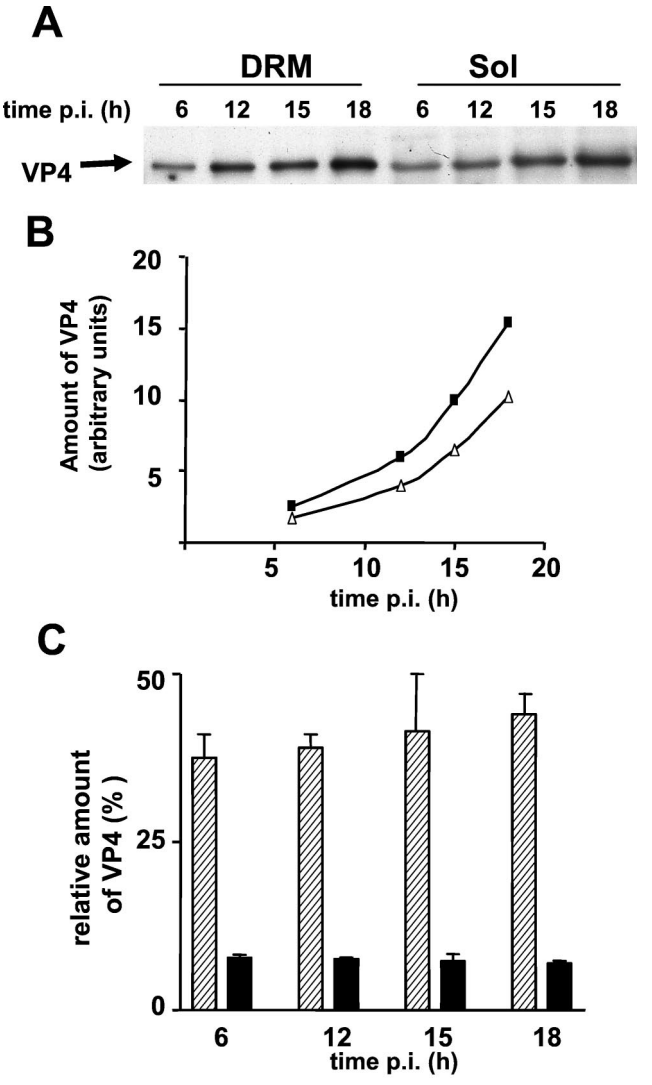

FIG. 5. VP4 is present and enriched in the DRM fraction. Flasks of Caco-2 cells (25 cm^2) were infected at 10 PFU/cell and incubated for different times p.i. Cells were then treated with Triton X-100, and DRM were prepared by flotation on an OptiPrep gradient. Fractions (1 ml) were collected. Fractions 4 and 5 accounted for the DRM fraction, and the bottom four fractions, containing 1% Triton X-100 and 40% OptiPrep, were pooled and accounted for the soluble fraction. (A) After TCA precipitation, 2% of the DRM (6.7 μg of protein) and 1% of the soluble fraction (48 μg of protein) were analyzed by Western blotting using an anti-VP4 antibody (monoclonal antibody 7.7). (B) Blots were quantified using Scion Image software. Black squares and white triangles, total amounts of VP4 in the soluble and DRM fractions, respectively. (C) Amounts of VP4 relative to the amounts of total protein present in soluble (black bars) and DRM (hatched bars) fractions at 18 h p.i.

that VP4 can directly interact with membranes resembling the rafts. It is important that in the absence of cholesterol the VP4-induced changes were not observed (not shown).

The other structural proteins of rotavirus later associate with microdomains. We demonstrated previously that in Caco-2 cells the entire virus was apically secreted and hypothesized that lipid rafts were responsible for this polarized targeting (30). Kinetic studies were undertaken determine if the

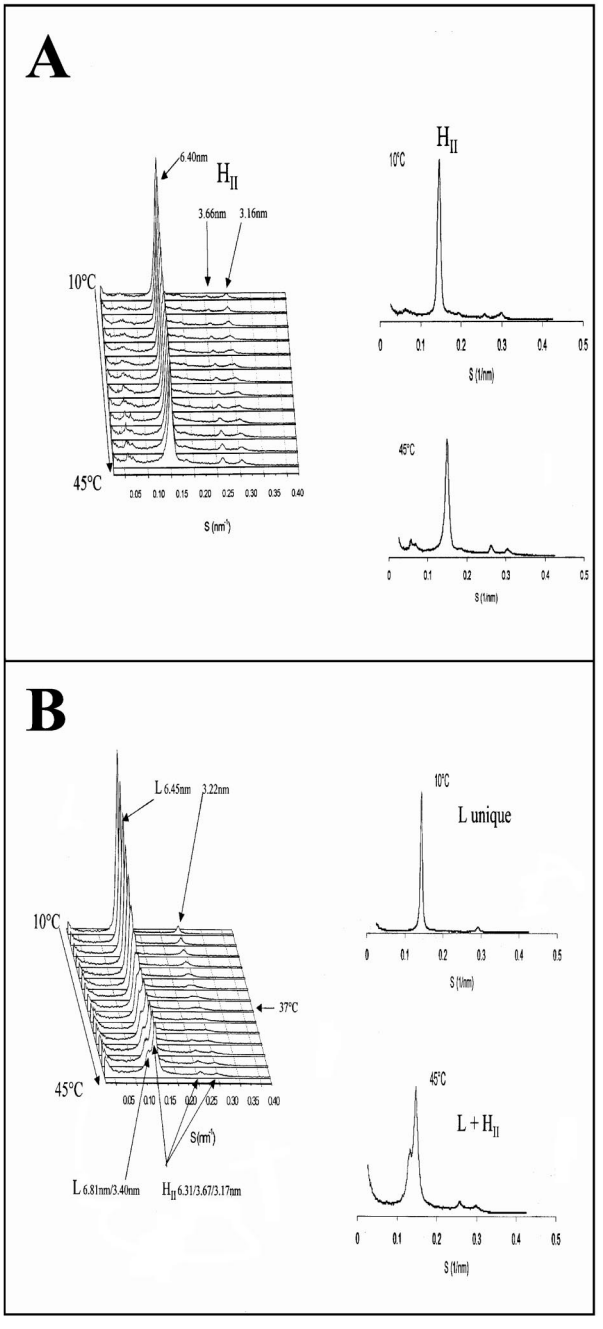

FIG. 6. Influence of virus protein VP4 on the phase behavior of a model lipid mixture. The lipid mixture used in these experiments contained phosphatidylethanolamine-phosphatidylserine-sphingomyelin-cholesterol (50/17/15/18 [mol/mol]). Lipids were fully hydrated at pH 8 in the presence of calcium (1 cation/100 lipids). (A) The lipid mixture adopts an inverted-hexagon arrangement characterized by a periodicity of 6.4 nm between 10 and 45°C. A trace of Pn3m-type cubic phase is detected in the small-angle area at the highest temperatures recorded. (B) In the presence of VP4 the lamellar phase (repeat distance, 6.45 nm) is preferred. Above 37°C the lamellar arrangement coexists with an inverted-hexagon phase (repeat distance, 6.31 nm).

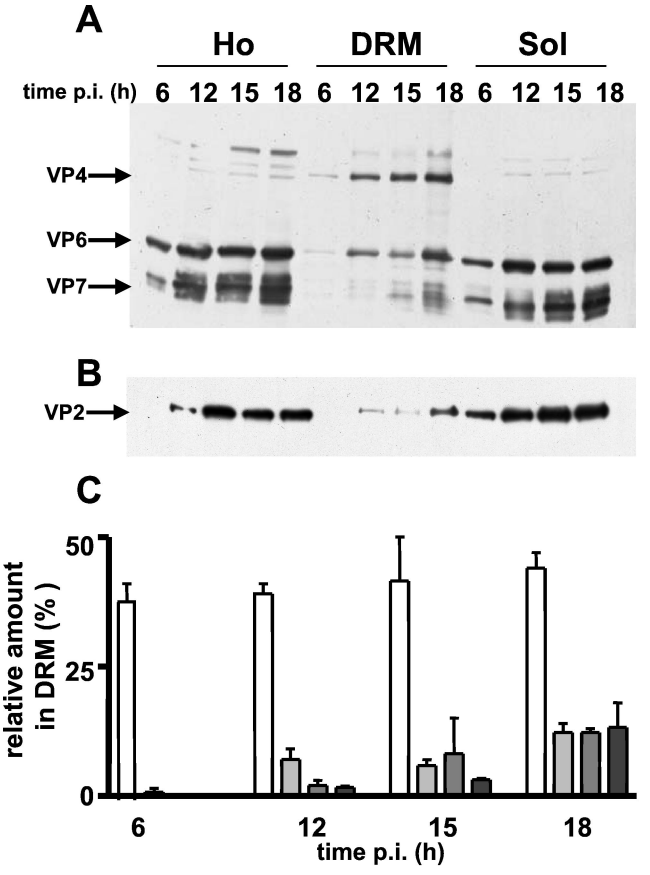

FIG. 7. The other virus structural proteins appeared progressively in the DRM fraction. Soluble (Sol) and DRM fractions were prepared as for Fig. 5 and were compared to crude homogenates (Ho). (A) Virus proteins detected by Western blotting using a polyclonal anti-RF antibody in total-homogenate, DRM, and soluble fractions at 6, 12, 15, and 18 h p.i. (note that the amounts of the samples loaded on the gel represented 0.5, 4, and 0.45% of total-homogenate, DRM, and soluble fractions, respectively, and that these values were used to normalize the percentages calculated for panel C). VP4, VP6, and VP7 are indicated. (B) VP2 was detected by Western blotting using a monoclonal anti-VP2 antibody. (note that the amounts of the samples loaded on the gel represented 0.5, 4, and 0.9% of total-homogenate, DRM, and soluble fractions, respectively, and that these values were used to normalize the percentages calculated for panel C). (C) Blots were quantified and normalized, and results (mean ± standard deviations of two independent determinations) are expressed as percentages of the viral proteins in the DRM fraction compared to their total amounts in whole-cell homogenate. White, light gray, medium gray, and dark gray bars, VP4, VP2, VP6, and VP7, respectively.

other structural proteins of rotavirus could associate with microdomains. Confluent Caco-2 cells were infected at 10 PFU/cell, and DRM were prepared at 6, 12, 15, and 18 h p.i. Viral proteins were analyzed in the homogenate and the soluble and DRM fractions. As expected after 6 h the total biosynthesis of viral proteins was low (Fig. 7A and B). The percentage of individual viral proteins associated with DRM was calculated from WBs by comparing the amount of each viral protein in this fraction to its total amount in the DRM plus soluble fractions or in homogenates. VP2, VP6, and VP7 were barely detectable in the DRM fraction at 6 h p.i. and started to be detectable after 12 h. At 18 h p.i. the structural viral proteins were found in the microdomains although the proportion of VP4 remained prominent. Quantification of blots showed an increased enrichment of proteins VP2, VP6 and VP7 with p.i. time. At 18 h p.i., the proportion of each individual viral pro-

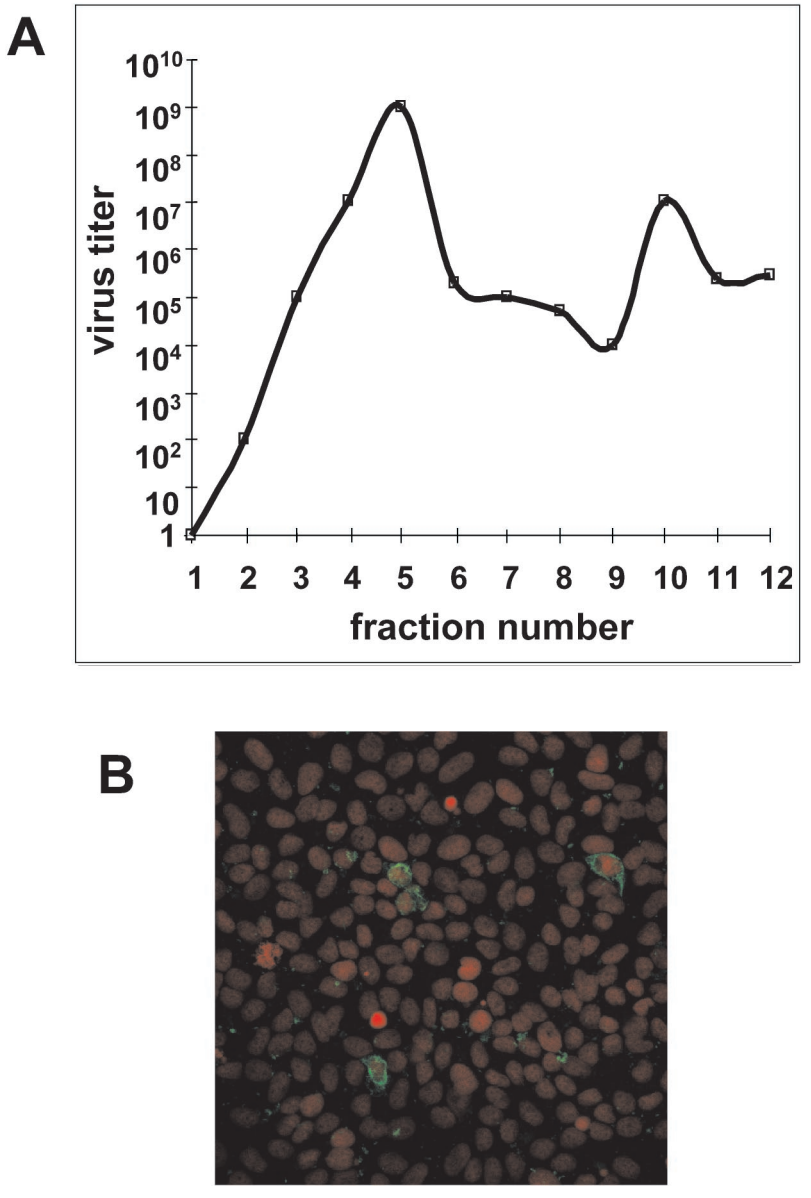

FIG. 8. Rafts prepared from infected cells contain infectious viral particles. (A) Quantification of virus-associated particles along the sucrose gradient. Caco-2 cells were infected at 10 PFU/cell and were collected 24 h p.i. Whole-cell homogenates were subjected to a sucrose gradient as described in Materials and Methods. Fractions were collected, and the rotavirus titer in each fraction was determined as previously described (40). The data are representative of three independent experiments. (B) Caco-2 cells were infected at 10 PFU/cell and were collected 24 h p.i. DRM were purified by flotation from these infected cells and used to infect MA 104 cells, which were screened by indirect IF for the presence of rotavirus using an anti-RF antibody and a secondary FITC-labeled anti-rabbit IgG antibody. Nuclei were stained with propidium iodide.

tein in DRM compared to its total amount in cells was about 10% (Fig. 7C). The presence of the structural proteins of rotavirus in DRM at late times p.i. strongly suggested the presence of the entire mature virus on these microdomains when assembly operates in Caco-2 cells, since in a previous work (30) we performed measurements that indicated that virion release started to be barely detectable at 12 h, slightly increased at 16 h p.i., and reached a plateau after 18 h p.i.

Rafts prepared from infected cells contain infectious viral particles. Association of the main viral structural proteins with rafts does not imply that mature infectious particles were assembled on these microdomains. To demonstrate this point, we used two complementary approaches. In the first one, we measured rotavirus titers in each of the fractions of the sucrose gradient used to purify DRM from infected Caco-2 cells. As shown in Fig. 8A, a large proportion of mature virus was recovered in fractions 4 and 5, which corresponded to DRM (Fig. 3 shows an example). Amounts of virus recovered in these two fractions exceeded by 2 orders of magnitude those found in other fractions in the gradient, thus indicating that infectious particles were enriched in DRM. In the second approach, DRM were purified by flotation from infected Caco-2 cells as described above and were used to infect MA 104 cells, which were screened for the presence of rotavirus by indirect IF using

a polyclonal anti-RF antibody. As shown in Fig. 8B DRM prepared from infected cells were able to promote rotavirus infection, thus indicating the presence of functional infectious particles in the DRM fraction.

Mature virions interact with model lipid membranes resembling rafts. To confirm that the entire virus interacts with rafts, additional X-ray diffraction experiments were performed. In these experiments, conducted in vitro, the purified mature viral particles, instead of purified recombinant VP4 protein, were mixed with the model lipid mixtures previously used (Fig. 6). Interestingly when rotavirus particles were added to the lipids, the phase equilibrium was also shifted to a lamellar arrangement characterized by a repeat distance of 6.77 nm (Fig. 9), similar to the L arrangement stabilized by VP4 (repeat distance, 6.8 nm). In a control experiment conducted in the absence of cholesterol no lamellar phase was observed in the presence or in the absence of virus (not shown), indicating that the interactions of virus with the lipid membranes were cholesterol dependent. These data strongly suggested that the mature infectious virus associated with rafts through a physical interaction that resembles the interaction of VP4 alone.

NSP4, a nonstructural protein involved in virus assembly, also associates with rafts. From the above results, it can be hypothesized that VP4 associated with rafts in the early phase of infection and that later the other structural proteins assembled in mature virions by using rafts as a platform. If rafts play a critical role as a platform to assemble neovirions, then NSP4, a nonstructural protein known to play a key role in the final steps of rotavirus assembly (62, 63), should associate with rafts at the time of virus formation. To explore this point, a kinetic study in which rafts were prepared from Caco-2 cells at 6, 12, and 18 h p.i. was performed. The presence of NSP4 was checked by Western blotting using a specific monoclonal antibody on both the soluble and the DRM fractions. As shown in Fig. 10 NSP4 was detected in the soluble but not DRM fractions as soon as 6 h p.i., a result that corroborates previous findings obtained with MA 104 cells (72). Interestingly, NSP4 became faintly detectable in the DRM fraction only at 12 h p.i. and was strongly expressed in microdomains at 18 h p.i., as observed above for virus structural proteins (Fig. 7).

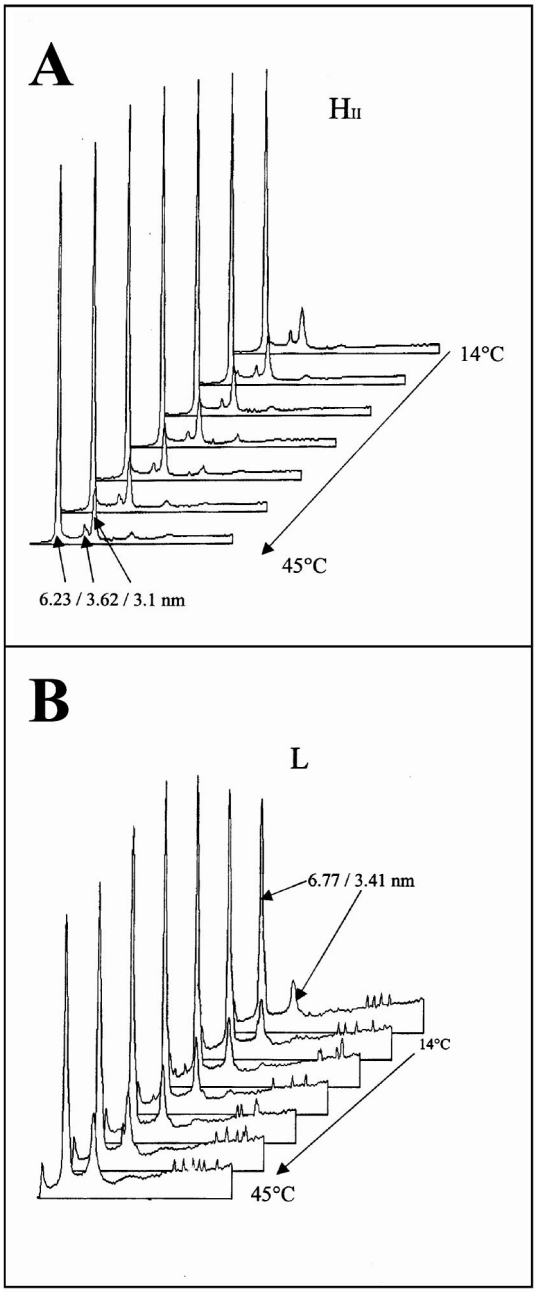

FIG. 9. Influence of virus particles on the phase behavior of a model lipid mixture. The lipid mixture used in these experiments contained phosphatidylethanolamine-phosphatidylserine-sphingomyelin-cholesterol (4/1/2/2 [mol/mol]). Lipids were fully hydrated in the presence of calcium (1 cation/1,000 lipids). (A) The quaternary mixture retains a single inverted hexagonal phase between 14 and 45°C (heating temperature scan rate, 2°C/min). The diffraction peaks point to the repeat distance (d) of 6.23 nm, with a second-order signal corresponding to the periodicity d:d/1:d/2:. . . . (B) When viral particles are added to the previous lipid mixture, the phase is changed to a single lamellar arrangement characterized by a repeat distance of 6.77 nm (6.77/3.41 for the periodicity 1/[1/2]).

DISCUSSION

In the present work we explored the interactions of VP4, the spike protein of rotavirus, with rafts in intestinal Caco-2 cells in order to better understand its role in the polarized targeting and the assembly process of this nonenveloped virus. Most of the studies on this topic concern enveloped viruses, such as influenza virus (53), human immunodeficiency virus (47), measles virus (66), and Ebola virus (8). Data on the membrane interactions of nonenveloped virus are scarce (37, 48). We show here for the first time that a nonenveloped virus is able to associate with membranes whose lipid composition indicates that they are authentic rafts through direct interaction of one of its structural proteins, namely, VP4. Our results likely correspond to a late event of virus maturation. They suggest that infectious virions are formed on rafts that act as a platform promoting virus assembly through a direct interaction with VP4.

How does VP4 interact with rafts? One of the most striking results of the present work is the demonstration that VP4, a cytosolically synthesized protein, directly interacts with lipid microdomains. An increasing number of proteins, including

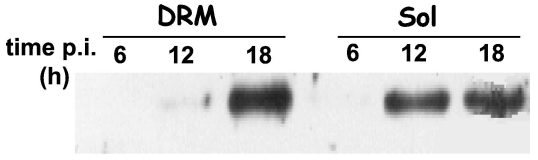

FIG. 10. Nonstructural protein NSP4 is associated with rafts at 18 h p.i. The soluble fraction and DRM were prepared as for Fig. 5. Two percent of the DRM and 0.5% of the soluble fraction were loaded on the gel. NSP4 was detected by Western blotting using a polyclonal anti-NSP4 antibody.

viral proteins, have been shown to interact with rafts, mostly through their transmembrane domains (32, 39, 54). It has also been shown that another viral protein reversibly associates with rafts through covalent lipid modifications, namely, poliovirus capsid protein VP4, whose myristoylation is responsible for its targeting to DRM (37). Although there are potential consensus sites for rotavirus VP4 acylation, this protein has never been shown to be acylated in vivo. This strongly suggests that VP4 should associate with rafts in an alternative way since this protein interacts directly but does not exhibit an obvious transmembrane domain or a GPI anchor and is not glycosylated (61). VP4 is a 776-amino-acid (aa) protein that presents some well-characterized signatures: a fusogenic domain (aa 383 to 405), a coiled-coil domain (aa 494 to 516), an integrin-interacting domain (aa 302 to 315), and a caveolin binding consensus sequence (aa 287 to 296). Recent data suggest that the fusogenic domains of viral proteins may be involved in in vitro interactions with membrane lipid models (25, 57). In line with these suggestions, it has been shown that VP4, together with VP7, promotes membrane fusion of virus with liposomes (45) and that VP4 is responsible for cell fusion from without through its fusogenic domain (15, 21). However, these observations point to a role of the fusogenic domain in rotavirus entry, i.e., a passage through the membrane rather than a simple interaction with membranes. VP4 also exhibits a caveolin binding domain (aa 287 to 296), which is a good candidate for interactions with rafts. However, since Caco-2 cells do not express caveolins (40), the involvement of this domain in our model seems to be unlikely. A final possibility is that VP4 interacts with rafts through its VP8* component, which is located on the N-terminal part of the molecule, oriented toward the exterior of the particle (13, 70). Interestingly it has been reported very recently that VP8* contains a galectin-like domain (P. R. Dormitzer, Z. Y. J. Sun, H. B. Greenberg, G. Wagner, and S. C. Harrison, Abstr. 20th Annu. Meet. Am. Soc. Virol., abstr. W 15-1, 2001), a result reminiscent of data indicating that several viruses that display a hemagglutinin domain, such as rotavirus VP4, have a lectin domain (10, 56, 65). Therefore it is possible that the lectin-like domain of VP8* carries a raft-interacting function, as already proposed for cellular glycoproteins en route to the apical membrane (16). Further experiments are needed to delineate if direct interaction of VP4 with sphingolipid-cholesterol-rich membranes and/or with glycosphingolipids is involved in rotavirus-raft interactions.

Where may VP4 interact with rafts? It is assumed that rafts play a key role in apical targeting in epithelial cells (58). Our results clearly demonstrate that VP4 association with rafts and its apical targeting are two related events. An unresolved aspect of this conclusion is to understand where a protein known to be synthesized in the cytoplasm may interact with rafts. After its cytoplasmic synthesis VP4 may associate with rafts already present on the apical plasma membrane. However it is not clear why VP4 specifically prefers the apically located microdomains. One possible explanation may rely on the fact that the lipid compositions of the apical and the basolateral domains are different (33, 64). We favor a second hypothesis, in which, after its synthesis in the cytoplasm, VP4 may rapidly attach to intracellular membranes en route to the apical surface. Interestingly such a mechanism has recently been proposed for a family of cellular cytosolic proteins named galectins, which, as already shown for rotavirus (30), reach the cell membrane through an atypical route bypassing the Golgi (26). More interestingly galectin 4, a member of this family, has been shown to reach the apical membrane of polarized cells through a Golgi-bypassing pathway thanks to its association with rafts (24). Since the VP8* core contains a galectin-like domain (Dormitzer et al., 20th Annu. Meet. Am. Soc. Virol.), it is tempting to speculate that VP4 may follow a pathway similar to the one described for galectin 4. If this mechanism holds true in Caco-2 cells, then it remains to find out the subcellular origin of rafts with which VP4 associates. In eucaryotic cells, rafts cannot be synthesized in the ER because of the lack of sphingolipid synthesis in this compartment, by contrast with yeasts, in which ER rafts have been characterized (43). It is assumed that rafts emerge from the Golgi and/or the trans-Golgi network (42), a location where neither VP4 nor entire rotavirus was detected (22, 30). Further studies are needed to define the precise origin of rafts that interact with VP4. These rafts may either derive from the retrograde transport between the Golgi apparatus and the ER or be part of another organelle located in the vicinity of the ER.

What are the consequences of our finding for rotavirus assembly? The present results are consistent with the view that rotavirus interacts with rafts through its spike protein, VP4, and suggest that these microdomains act as a platform for virus final assembly. The delayed association of other rotavirus structural proteins and the presence of NSP4 within rafts at the time of virus assembly strongly argue for such a mechanism. The fact that the proportions of virus structural proteins in rafts, except for VP4, remain low is also in agreement with the fact that virus assembly is a transient phenomenon, which is rapidly followed by the dissociation of mature viruses from the rafts and their secretion. In the classical model of rotavirus assembly, it is assumed that the whole process takes place into the ER. How may rafts play a role since until now no raft in the ERs of mammalian cells has been described? This question leads us to propose a new model of rotavirus assembly in which the final part of the process, namely, VP4 incorporation into preformed particles, takes place in an extrareticular location. Rafts then provide a platform that already contains VP4 and that upon NSP4 attachment incorporates VP7 and the other structural proteins. The present results favor this later view, and current investigations are dedicated to the identification of the compartment that contains rafts and that will interact with the ER to accomplish this final assembly step.

ACKNOWLEDGMENTS

C. Sapin and O. Colard contributed equally to the work.

We thank Hans Peter Hauri, Suzanne Maroux, and John Taylor for providing antibodies. Annie Charpilienne was present throughout the work, and her kind help with rotavirus technologies was very useful. Philippe Fontanges took care of the confocal microscope, which gave us many interesting pictures. Thanks to Karine Gherdi for secretarial work.

This work was supported by grants from the research ministry of France (PRFMMIP), institutional funds from INSERM and Université Pierre et Marie Curie (Paris VI, France), and grants from the FRM (IC.34 to G. Trugnan) and ARC (no. 9367 to G. Trugnan).

REFERENCES

1. **Ait Slimane, T., C. Lenoir, V. Bello, J.-L. Delaunay, J. W. Goding, S. Chwetzoff, M. Maurice, J. A. M. Fransen, and G. Trugnan.** 2001. The cytoplasmic/transmembrane domain of dipeptidyl peptidase IV, a type II glycoprotein, contains an apical targeting signal that does not specifically interact with rafts. Exp. Cell Res. **270:**45–55.
2. **Anonymous.** 1999. Rotavirus vaccines. Wkly. Epidemiol. Rec. **74:**33–38.
3. **Blank, M. L., M. Robinson, and F. Snyder.** 1984. Novel quantitative method for determination of molecular species of phospholipids and diglycerides. J. Chromatogr. **298:**473–482.
4. **Bligh, E. G., and W. J. Dyer.** 1959. A rapid method of total lipid extraction and purification. Can. J. Biochem. Physiol. **37:**911–917.
5. **Boulin, C., R. Kempf, A. Gabriel, M. Koch, and S. McLaughlin.** 1986. Data appraisal, evaluation and display for synchrotron radiation experiments: hardware and software. Nucl. Instrum. Methods **249:**399–409.
6. **Brown, D. A., and J. K. Rose.** 1992. Sorting of GPI-anchored proteins to glycolipid-enriched membrane subdomains during transport to the apical cell surface. Cell **68:**533–544.
7. **Centers for Disease Control and Prevention.** 1999. Withdrawal of rotavirus vaccine recommendation. JAMA **282:**2113–2114.
8. **Chan, S. Y., C. J. Empig, F. J. Welte, R. F. Speck, A. Schmaljohn, J. F. Kreisberg, and M. A. Goldsmith.** 2001. Folate receptor-alpha is a cofactor for cellular entry by Marburg and Ebola viruses. Cell **106:**117–126.
9. **Chan, W. K., K. S. Au, and M. K. Estes.** 1988. Topography of the simian rotavirus nonstructural glycoprotein (NS28) in the endoplasmic reticulum membrane. Virology **164:**435–442.
10. **Chen, J., K. H. Lee, D. A. Steinhauer, D. J. Stevens, J. J. Skehel, and D. C. Wiley.** 1998. Structure of the hemagglutinin precursor cleavage site, a determinant of influenza pathogenicity and the origin of the labile conformation. Cell **95:**409–417.
11. **Darmoul, D., M. Lacasa, L. Baricault, D. Marguet, C. Sapin, P. Trotot, A. Barbat, and G. Trugnan.** 1992. Dipeptidyl peptidase IV (CD 26) gene expression in enterocyte-like colon cancer cell lines HT-29 and Caco-2. Cloning of the complete human coding sequence and changes of dipeptidyl peptidase IV mRNA levels during cell differentiation. J. Biol. Chem. **267:**4824–4833.
12. **Delorme, C., H. Brussow, J. Sidoti, N. Roche, K. A. Karlsson, J. R. Neeser, and S. Teneberg.** 2001. Glycosphingolipid binding specificities of rotavirus: identification of a sialic acid-binding epitope. J. Virol. **75:**2276–2287.
13. **Dormitzer, P. R., H. B. Greenberg, and S. C. Harrison.** 2001. Proteolysis of monomeric recombinant rotavirus VP4 yields an oligomeric VP5* core. J. Virol. **75:**7339–7350.
14. **Estes, M. K.** 1996. Rotavirus and their replication, p. 1625–1655. *In* B. N. Fields, D. M. Knipe, and P. M. Howley (ed.), Fields virology, 3rd ed. Lippincott-Raven Publishers, Philadelphia, Pa.
15. **Falconer, M. M., J. M. Gilbert, A. M. Roper, H. B. Greenberg, and J. S. Gavora.** 1995. Rotavirus-induced fusion from without in tissue culture cells. J. Virol. **69:**5582–5591.
16. **Fiedler, K., R. G. Parton, R. Kellner, T. Etzold, and K. Simons.** 1994. VIP36, a novel component of glycolipid rafts and exocytic carrier vesicles in epithelial cells. EMBO J. **13:**1729–1740.
17. **Fogh, J., T. Orfeo, J. Tiso, F. E. Sharkey, J. M. Fogh, and W. P. Daniels.** 1980. Twenty-three new human tumor lines established in nude mice. Exp. Cell Biol. **48:**229–239.
18. **Gajardo, R., P. Vende, D. Poncet, and J. Cohen.** 1997. Two proline residues are essential in the calcium-binding activity of rotavirus VP7 outer capsid protein. J. Virol. **71:**2211–2216.
19. **Gamble, W., M. Vaughan, H. Kruth, and J. Avigan.** 1978. Procedure for determination of free and total cholesterol in micro- and nanogram amounts suitable for studies with cultured cells. J. Lipid Res. **19:**1068–1070.
20. **Garcia, M., C. Mirre, A. Quaroni, H. Reggio, and A. Le Bivic.** 1993. GPI-anchored proteins associate to form microdomains during their intracellular transport in Caco-2 cells. J. Cell Sci. **104:**1281–1290.
21. **Gilbert, J. M., and H. B. Greenberg.** 1998. Cleavage of rhesus rotavirus VP4 after arginine 247 is essential for rotavirus-like particle-induced fusion from without. J. Virol. **72:**5323–5327.
22. **Gonzalez, R. A., R. Espinosa, P. Romero, S. Lopez, and C. F. Arias.** 2000. Relative localization of viroplasmic and endoplasmic reticulum-resident rotavirus proteins in infected cells. Arch. Virol. **145:**1963–1973.
23. **Guerrero, C. A., S. Zarate, G. Corkidi, S. Lopez, and C. F. Arias.** 2000. Biochemical characterization of rotavirus receptors in MA104 cells. J. Virol. **74:**9362–9371.
24. **Hansen, G. H., L. Immerdal, E. Thorsen, L. L. Niels-Christiansen, B. T. Nystrom, E. J. Demant, and E. M. Danielsen.** 2001. Lipid rafts exist as stable cholesterol-independent microdomains in the brush border membrane of enterocytes. J. Biol. Chem. **276:**32338–32344.
25. **Hristova, K., W. C. Wimley, V. K. Mishra, G. M. Anantharamiah, J. P. Segrest, and S. H. White.** 1999. An amphipathic alpha-helix at a membrane interface: a structural study using a novel X-ray diffraction method. J. Mol. Biol. **290:**99–117.
26. **Hughes, R. C.** 1999. Secretion of the galectin family of mammalian carbohydrate-binding proteins. Biochim. Biophys. Acta **1473:**172–185.
27. **Ikonen, E.** 2001. Roles of lipid rafts in membrane transport. Curr. Opin. Cell Biol. **13:**470–477.
28. **Iwabushi, K., K. Handa, and S. Hakomori.** 1998. Separation of "glycosphingolipid signaling domain" from caveolin-containing membrane fraction in mouse melanoma B16 cells and its role in cell adhesion coupled with signaling. J. Biol. Chem. **273:**33766–33773.
29. **Jourdan, N., J. P. Brunet, C. Sapin, A. Blais, J. Cotte-Laffitte, F. Forestier, A. M. Quero, G. Trugnan, and A. L. Servin.** 1998. Rotavirus infection reduces sucrase-isomaltase expression in human intestinal epithelial cells by perturbing protein targeting and organization of the microvillar cytoskeleton. J. Virol. **72:**7228–7236.
30. **Jourdan, N., M. Maurice, D. Delautier, A. M. Quero, A. L. Servin, and G. Trugnan.** 1997. Rotavirus is released from the apical surface of cultured human intestinal cells through nonconventional vesicular transport that bypasses the Golgi apparatus. J. Virol. **71:**8268–8278.
31. **Kabcenell, A. K., M. S. Poruchynsky, A. R. Bellamy, H. B. Greenberg, and P. H. Atkinson.** 1988. Two forms of VP7 are involved in assembly of SA11 rotavirus in the endoplasmic reticulum. J. Virol. **62:**2929–2941.
32. **Kundu, A., R. T. Avalos, C. M. Sanderson, and D. P. Nayak.** 1996. Transmembrane domain of influenza virus neuraminidase, a type II protein, possesses an apical sorting signal in polarized MDCK cells. J. Virol. **70:**6508–6515.
33. **Le Bivic, A., C. Le Grimellec, C. Wolf, and G. Trugnan.** 2000. Interactions membranaires lipides-protéines et polarité épithéliale: macrodomaines, microdomaines et fonctions polarisées, p. 13–24. *In* C. Clerici and G. Friedlander (ed.), Biologie et pathologie des epithéliums. EDK, Paris, France.
34. **L'Haridon, R., and R. Scherrer.** 1976. In vitro culture of rotavirus associated with neonatal calf scours. Ann. Rech. Vet. **7:**373–381.
35. **London, E., and D. A. Brown.** 2000. Insolubility of lipids in Triton X-100: physical origin and relationship to sphingolipid/cholesterol membrane domains (rafts). Biochim. Biophys. Acta **1508:**182–195.
36. **Maass, D. R., and P. H. Atkinson.** 1990. Rotavirus proteins VP7, NS28, and VP4 form oligomeric structures. J. Virol. **64:**2632–2641.
37. **Martin-Belmonte, F., J. A. Lopez-Guerrero, L. Carrasco, and M. A. Alonso.** 2000. The amino-terminal nine amino acid sequence of poliovirus capsid VP4 protein is sufficient to confer N-myristoylation and targeting to detergent-insoluble membranes. Biochemistry **39:**1083–1090.
38. **Masrar, H., G. Béréziat, and O. Colard.** 1990. Very high proportion of disaturated molecular species in rat platelet diacyl-glycerophosphocholine: involvement of CoA-dependent transacylation reactions. Arch. Biochem. Biophys. **281:**116–123.
39. **Melikyan, G. B., S. Lin, M. G. Roth, and F. S. Cohen.** 1999. Amino acid sequence requirements of the transmembrane and cytoplasmic domains of influenza virus hemagglutinin for viable membrane fusion. Mol. Biol. Cell **10:**1821–1836.
40. **Mirre, C., L. Monlauzeur, M. Garcia, M. H. Delgrossi, and A. Le Bivic.** 1996. Detergent-resistant membrane microdomains from Caco-2 cells do not contain caveolin. Am. J. Physiol. **271:**C887–C894.
41. **Montixi, C., C, Langlet, A. M. Bernard, J. Thimonier, C. Dubois, M. A. Wurbel, J. P. Chauvin, M. Pierres, and H. T. He.** 1998. Engagement of T cell receptor triggers its recruitment to low-density detergent-insoluble membrane domains. EMBO J. **17:**5334–5348.
42. **Mora, R., V. L. Bonilha, A. Marmorstein, P. E. Scherer, D. Brown, M. P. Lisanti, and E. Rodriguez-Boulan.** 1999. Caveolin-2 localizes to the Golgi complex but redistributes to plasma membrane, caveolae, and rafts when co-expressed with caveolin-1. J. Biol. Chem. **274:**25708–25717.
43. **Muniz, M., P. Morsomme, and H. Riezman.** 2001. Protein sorting upon exit from the endoplasmic reticulum. Cell **104:**313–320.
44. **Naim, H. Y., E. Ehler, and M. A. Billeter.** 2000. Measles virus matrix protein specifies apical virus release and glycoprotein sorting in epithelial cells. EMBO J. **19:**3576–3585.
45. **Nandi, P., A. Charpilienne, and J. Cohen.** 1992. Interaction of rotavirus particles with liposomes. J. Virol. **66:**3363–3367.
46. **Nejmeddine, M., G. Trugnan, C. Sapin, E. Kohli, L. Svensson, S. Lopez, and J. Cohen.** 2000. Rotavirus spike protein VP4 is present at the plasma membrane and is associated with microtubules in infected cells. J. Virol. **74:**3313–3320.
47. **Nguyen, D. H., and J. E. Hildreth.** 2000. Evidence for budding of human immunodeficiency virus type 1 selectively from glycolipid-enriched membrane lipid rafts. J. Virol. **74:**3264–3272.

48. **Pelkmans, L., J. Kartenbeck, and A. Helenius.** 2001. Caveolar endocytosis of simian virus 40 reveals a new two-step vesicular-transport pathway to the ER. Nat. Cell Biol. **3:**473–483.
49. **Poruchynsky, M. S., and P. H. Atkinson.** 1991. Calcium depletion blocks the maturation of rotavirus by altering the oligomerization of virus-encoded proteins in the endoplasmic reticulum. J. Virol. **65:**4720–4727.
50. **Poruchynsky, M. S., C. Tyndall, G. W. Both, F. Sato, A. R. Bellamy, and H. Atkinson.** 1985. Deletions into an NH2-terminal hydrophobic domain result in secretion of rotavirus VP7, a resident endoplasmic reticulum membrane glycoprotein. J. Cell Biol. **101:**2199–2209.
51. **Rietveld, A., and K. Simons.** 1998. The differential miscibility of lipids as the basis for the formation of functional membrane rafts. Biochim. Biophys. Acta **1376:**467–479.
52. **Roseto, A., R. Scherrer, J. Cohen, M. C. Guillemin, A. Charpilienne, C. Feynerol, and J. Peries.** 1983. Isolation and characterization of anti-rotavirus immunoglobulins secreted by cloned hybridoma cell lines. J. Gen. Virol. **64:**237–240.
53. **Scheiffele, P., A. Rietveld, T. Wilk, and K. Simons.** 1999. Influenza viruses select ordered lipid domains during budding from the plasma membrane. J. Biol. Chem. **274:**2038–2044.
54. **Scheiffele, P., M. G. Roth, and K. Simons.** 1997. Interaction of influenza virus haemagglutinin with sphingolipid-cholesterol membrane domains via its transmembrane domain. EMBO J. **16:**5501–5508.
55. **Schneiter, R., B. Brugger, R. Sandhoff, G. Zellnig, A. Leber, M. Lampl, K. Athenstaedt, C. Hrastnik, S. Eder, G. Daum, F. Paltauf, F. T. Wieland, and S. D. Kohlwein.** 1999. Electrospray ionisation tandem mass spectrometry (ESI-MS/MS) analysis of the lipid molecular species composition of yeast subcellular membranes reveals acyl-chain-based sorting/remodeling of distinct molecular species en route to the plasma membrane. J. Cell Biol. **146:**741–754.
56. **Shaw, A. L., R. Rothnagel, D. Chen, R. F. Ramig, W. Chiu, and B. V. Prasad.** 1993. Three-dimensional visualization of the rotavirus hemagglutinin structure. Cell **74:**693–701.
57. **Siegel, D. P., and R. M. Epand.** 2000. Effect of influenza hemagglutinin fusion peptide on lamellar/inverted phase transitions in dipalmitoleoylphosphatidylethanolamine: implications for membrane fusion mechanisms. Biochim. Biophys. Acta **1468:**87–98.
58. **Simons, K., and E. Ikonen.** 1997. Functional rafts in cell membranes. Nature **387:**569–572.
59. **Starkey, W. G., J. Collins, T. S. Wallis, G. J. Clarke, A. J. Spencer, S. J. Haddon, M. P. Osborne, D. C. Candy, and J. Stephen.** 1986. Kinetics, tissue specificity and pathological changes in murine rotavirus infection of mice. J. Gen. Virol. **67:**2625–2634.
60. **Suzuki, H.** 1996. A hypothesis about the mechanism of assembly of double-shelled rotavirus particles. Arch. Virol. Suppl. **12:**79–85.
61. **Taniguchi, K., T. Urasawa, and S. Urasawa.** 1994. Species specificity and interspecies relatedness in VP4 genotypes demonstrated by VP4 sequence analysis of equine, feline, and canine rotavirus strains. Virology **200:**390–400.
62. **Taylor, J. A., J. A. O'Brien, V. J. Lord, J. C. Meyer, and A. R. Bellamy.** 1993. The RER-localized rotavirus intracellular receptor: a truncated purified soluble form is multivalent and binds virus particles. Virology **194:**807–814.
63. **Taylor, J. A., J. A. O'Brien, and M. Yeager.** 1996. The cytoplasmic tail of NSP4, the endoplasmic reticulum-localized non-structural glycoprotein of rotavirus, contains distinct virus binding and coiled coil domains. EMBO J. **15:**4469–4476.
64. **van Meer, G., and K. Simons.** 1988. Lipid polarity and sorting in epithelial cells. J. Cell. Biochem. **36:**51–58.
65. **Vijayan, M., and N. Chandra.** 1999. Lectins. Curr. Opin. Struct. Biol. **9:**707–714.
66. **Vincent, S., D. Gerlier, and S. N. Manie.** 2000. Measles virus assembly within membrane rafts. J. Virol. **74:**9911–9915.
67. **Whitaker, A. M., and C. J. Hayward.** 1985. The characterization of three monkey kidney cell lines. Dev. Biol. Stand. **60:**125–131.
68. **Wolf, C., K. Koumanov, B. Tenchov, and P. Quinn.** 2001. Cholesterol favors phase separation of sphingomyelin. Biophys. Chem. **89:**163–172.
69. **Xu, A., A. R. Bellamy, and J. A. Taylor.** 2000. Immobilization of the early secretory pathway by a virus glycoprotein that binds to microtubules. EMBO J. **19:**6465–6474.
70. **Yeager, M., K. A. Dryden, N. H. Olson, H. B. Greenberg, and T. S. Baker.** 1990. Three-dimensional structure of rhesus rotavirus by cryoelectron microscopy and image reconstruction. J. Cell Biol. **110:**2133–2144.
71. **Zhang, J., A. Pekosz, and R. A. Lamb.** 2000. Influenza virus assembly and lipid raft microdomains: a role for the cytoplasmic tails of the spike glycoproteins. J. Virol. **74:**4634–4644.
72. **Zhang, M., C. Q. Zeng, A. P. Morris, and M. K. Estes.** 2000. A functional NSP4 enterotoxin peptide secreted from rotavirus-infected cells. J. Virol. **74:**11663–11670.